ISSN No:-2456-2165

CFD Modeling and Approaches for Calculating the Losses of a Subsea Pipeline Transporting High-Pressurized Fluid

Joseph Amponsah[1*],
[*1]Cape Coast Technical University, Department of Mechanical Engineering

Mary Aboagye[3]
[3]University of Mines and Technology, Department of Petroleum and Natural Gas Engineering

Gertrude Mensah[2],
[2]University of Ghana, Department of Marketing and Entrepreneurship

Samuel Terkper Kwasi Tetteh[4]
[4]Cape Coast Technical University, Department of Mechanical Engineering

Abstract:- This research delves into the complex dynamics of high-pressure, hot, and dynamic liquids flowing through piping systems. To better understand the various factors that affect the torsional vibration of these liquids, the study uses a coupled nonlinear partial differential equation to analyze generating variables such as fluid flow heat flux, mass ratio, pipe thickness, internal pressurization, vertical motion, longitudinal direction kinetic energy of the inner fluid, and cross-sectional area change. The ANSYS CFD R2022a software is used to simulate the model, and a three-dimensional model is used to investigate the dynamic behavior of the thin pipe. The numerical modal analysis is performed in the configuration of fluid-structure interaction, and the study also examines the vibratory behavior of the fluid-conveying pipe. The results indicate that the velocity was 7.5% lower in the pipe with plaque model than in the normal pipe model, while pressure and WSS were 94.9% and 74.41% higher, respectively. The study also conducts parametric studies on the effect of temperature, pressure drop, and velocity change on the frequencies. Additionally, the research suggests that a gas column input signal exists in the pipe, which can cause severe vibration when it comes into contact with unreasonable vibration. This study highlights the importance of determining the ideal design for pipes to restore their usual functions and avoid excessive vibration.

Keywords: *Exploration; K-ε model; ANSYS Computational Fluid Dynamic; CFX Code; Vibration.*

➢ *Graphical Abstracts:*

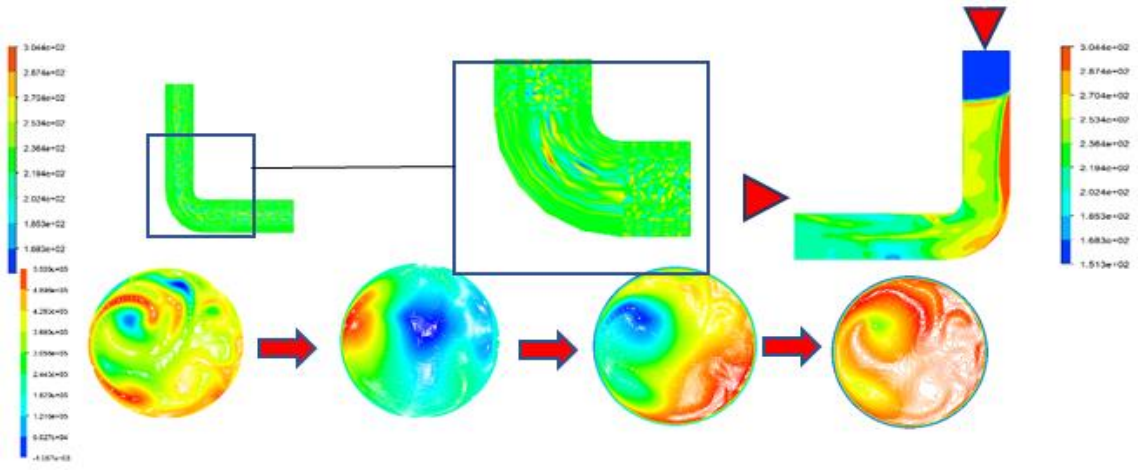

➢ *Nomenclature:*

CFX	Computational Fluid Dynamics
WSS	Welded Special Sections
API-5L	Specification for Line Pipe
OD	Outer Diameter

ISSN No:-2456-2165

I. INTRODUCTION

The research into the issue of pipe vibrations under the internal flow is highly fascinating. In most cases, pipes are subjected to vibrations caused by rotary equipment such as pumps, and compressors, or the wind force generates tensions in pipe sections, which in certain situations can lead the pipe material to break. Therefore, the requirement arises and is then deployed to examine the vibratory analysis of an undersea pipeline conveying fluid utilizing CFX. From literature reference made by [1], stated that Padoussis publish a book that collated all studies from various experiments relating to pipe vibrations under internal flow and represented them in linear and non-linear equations. They highlighted the analytical and experimental approach comparison made by Padoussis, and the variables influencing this behavior in geometrics and physics [2]. The book comprises more than 40 investigations and has served as a reference for any researcher on this topic. Some of Padoussi's research, ancient is concerned with the idea of instabilities (static instability and dynamic instability).

As offshore hydrocarbon resources are exploited, pipelines are used for a variety of purposes [3]. Pipeline bundles, water injection or chemical injection lines, and underwater pipeline mechanical design often involves taking into account several variables. The trapped liquids are the cause of the internal pressure. The pipeline will yield if the resulting stress on the pipe wall is too high. Additionally, there is external pressure on account of the hydrostatic and hydrodynamic forces acting on the pipeline. The type of sand and bottom shape both affect pipeline stability.

A pipeline constructed on an uneven seabed often creates a free space instead of fitting into the curvature of the seafloor. Expansion stress is brought on by the discrepancy between the pipeline's installation temperature and operational temperature. [4]. The pipeline's route is a significant aspect that might directly affect the cost and viability of a project. This might influence technical concerns like excessive water depth, the existence of geohazards, or geopolitical issues like national boundaries, for example. Furthermore, as pipeline routes penetrate continental slopes to abyssal or deep ocean depths, these issues often become more obvious. [5].

In another study conducted by [6,7], they use new analytical formulas to calculate the critical flow velocity inside a fixed-free tube on an elastic foundation. This was done using the [8] method and the same search for the boundary conditions: pinned-pinned and clamped [9]. They examined the impact of boundary conditions on the instability of one-dimensional systems [6,10]. The importance of the issue of instability and its influence on industrial life needs a lot of investigation and analysis. [11,12], also evaluated the influence of elastic foundations of the Pasternak type on the critical velocity of a fluid-conveying pipe. The Pasternak Winkler model was used in the same work by [5,11].

Similarly, the analytical method was adopted in most research (Galerkin method). While others used analytical methods to study the vibration of pipes with an internal flow such as the differential quadrature method [7,13], the differential transformation method [14], and the generalized integral transform technique [15]. The aforementioned approaches produce significant and beneficial results; however, Liquid fluids are delivered over the surface - or underground-based pipelines and may sometimes be at high heat, or above air pressure. Pipes are used in oil and gas activities, both onshore and offshore, to transport products or petroleum from one location to another. Because exploration for oil and gas and production is taking place in ultra-deep offshore waters, design engineers in the energy sector are concerned about the pipelines' capacity to withstand harsh working conditions.

II. METHOD AND MATERIALS

The available software to be used in this analysis is ANSYS Fluent version 2022 R1, which will be used to model the 3D underwater pipe computational flow in a high pressurize mixing profile. Table 1. Shows the various materials, and parameters used in this research. The simulation will make use of a 3D model of the pipe, and the analysis of the flows will involve use of steady-state assumptions. High pressure is believed to have a density of 1050 kg/m^3, in this research, the sample had a viscosity of 0.006 Pa and a capacity for the heat of 4100 J/kg K. The Gaussian distribution ratio of 0.01, Bulk modulus of 1.5 MPa, and a rising profile were found in the pipe. CFD was performed on the following model studies: Steady-State Vibrations, Fluid-carrying annular pipe dynamics, and Analysis of Transient Vibration. Each model's average pressure (Pa) and velocity (ms^{-1}) measurements will be determined additionally, it is believed that the mean fluid wall shear stress, WSS (Pa), will be measured.

Table 1 Values used for Simulation

Description	Value used
Material density of pipes	1050 kg/m^3
Fluid density within the pipe	977kg/m3
Pipe material elasticity modulus	2e$^+$11N/m2
Soil modulus of deformation	0.1N/m
Length of pipe	4000mm
External diameter of the pipe	200mm
The internal diameter of the pipe	180mm
Moment of inertia	0.42384m2
The velocity of fluid flowing in a pipe	2-15m/sec

Inlet temperature	200-400celcius
Pressure	0-4Mpa

➢ *Numerical Formulation and Governing Equations:*

The incompressible and Newtown liquids used in this investigation are presumable or known to be used in this research. The equational approach uses the Navier-Stokes equation and the convection-diffusion formulas, which are useful for steady-state equation analysis and incompressible fluid used in this research.

The fluid in this steady is described by the use of the continuity equation.

$$\nabla \cdot u = 0$$
$$\rho(u \cdot \nabla u) = -\nabla P + \nabla \cdot [\mu - \{\nabla u) + (\nabla u)^{\mathrm{T}}\}] \quad 1$$

Here, p stands for pressure, s for velocity profile, d for density, and u for the vector of 3D velocities (m s^{-1}) (kg m^{-3}). The well-known Navier-Stokes equation may be used to represent Newtonian fluids (fluids with a state of continual viscosity) in this situation.

Convection-diffusion equations and the Navier-Stokes equation;

$$\rho(\mathrm{u} \cdot \nabla \mathrm{u}) = -\nabla \mathrm{P} + \mu \nabla 2\mathrm{u} \quad 2$$

$$\rho \frac{DV}{Dt} = \rho g - \nabla p + \mu \nabla^2 V \quad 3$$

Applying the continuity equation, as well as boundary conditions, a result is sought for the unknowns, where p, u, v, and w. If the issue involves thermal contact, the governing equations must also be taken into account. The Navier-Stokes equations can only be analytically solved in a small number of specific instances, despite this approximation.

$$K = \mu_\infty + \delta\mu \exp\left(-\left(1 + \frac{\gamma}{a}\right)\exp\left(\frac{-b}{\gamma}\right)\right)$$
$$n = n_\infty - \delta n \exp\left(-\left(1 + \frac{\gamma}{c}\right)\exp\left(\frac{-d}{\gamma}\right)\right) \quad 4$$

where $\mu\infty$ = 0.00645 Pa s, $n\infty$ = 2.0, $\delta\mu$ = 0.3, δn = 0.35, a = 60, b = 2.9, c = 60 and d = 4

➢ *Conditions at the Boundary, Geometrical Features and Reynolds Number:*

Because several simultaneous phenomena must be considered when describing a vibration analysis fluid motion, several simultaneous phenomena that must be taken into account when describing the motion of a microfluidics fluid in the pipe, it is typical to utilize a 3D model parameter to convey which phenomenon is dominant. The Reynolds number, Re, is by far the parameter that is referenced the most.

The proportion of viscosity to inertial forces determines this characteristic. As a result, laminar flow regimes are defined by low Reynolds numbers (2000), and turbulent flow is defined by high Reynolds numbers (> 3000). Other dimensionless metrics include the Péclet number, which expresses the proportion of convection to diffusion. The diagram below shows the 3D representation of the pipe channel. By default, the external diameter = 200m, its internal diameter = 180mm, its length = 400mm, the velocity of water in pipe = 2-10m/s, and its axial length is X0 = 200 m. A temperature of 373-573k was considered. At the microchannel's intake, a boundary of zer'-gauge pressure is used. The walls have a no-slip border condition imposed on them.

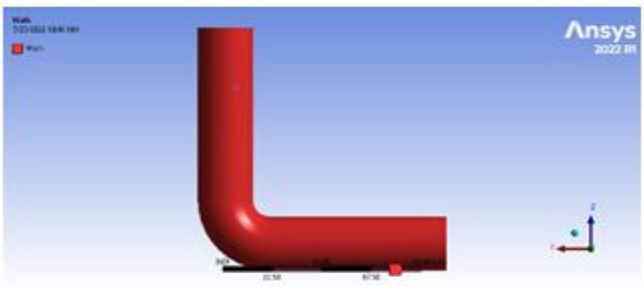

Fig 1 Pipe Geometry and Boundary Condition

At the flow region's outflow, a boundary condition is established based on the already existing experimental observations flow rate Q (L min-1). The fluid flow rate balanced equation is

$$Q = \frac{0.12AD_hY_0}{\lambda} \quad 5$$

where 0 (s-1.2) is the overall flow velocity, A (m2) is the concept of multi-area, Dh (m) is the fluid diameter, and A, Dh, and are derived using the formulas below.)

$$A = Y_0 Z_0$$
$$D_h = \frac{2A}{Y_0 + Z_0}$$
$$\lambda = \frac{24}{[(1 - 0.351Y_0/Z_0)(1 + Y_0/Z_0)]^2} \quad 6$$

The preceding enables Laminar or turbulent flow rates in a stream are determined by the Reynolds number, an incompressible group., to be calculated. For a Nanofluid flow, the Reynolds number is given by

$$Re = \frac{D_h b^2 Q}{\mu A} \quad 7$$

➢ *Boundary Conditions:*

Generally, carbon steel"is utilized for pipes beneath the sea. The 2000 publication of API-5L, "Specification for Line "ipe," contains standard spec"fications. API-5L grades B to X80 cover sheets of steel with an outer diameter (OD) ranging from 4.5 to 80 inches. Table 1 displays the tensile strength parameters by API-5L. In general, X65 is the most

popular steel grade for deep-water subsea pipes because it is inexpensive and can be welded with acceptable practices [14]. The pipe material chosen for this project was API 5L X65.

➢ *Grid Independence T"st:*

Using the test used to check the test that is discussed in existing research, the grid size employed in this study is 1.1 million to 3.9 million or fewer cells were used, and both the fluid flow and mixture index were affected by the various cell numbers and studied. The grid independence test was conducted using microchannels with two distinct shapes. It was discovered that a grid with around 3.9 million cells was enough. The simulations described in this research employed a grid with a comparable grid quality.

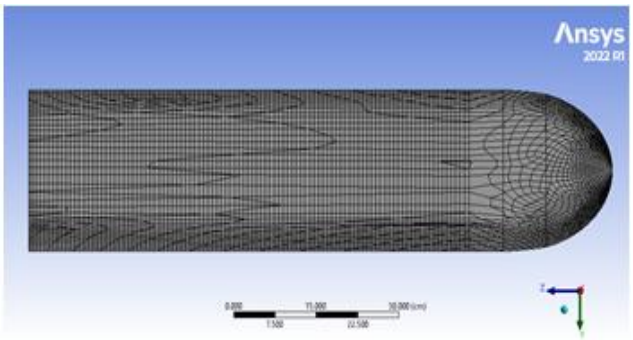

Fig 2 A) Cross-Section of the Final Volume Mesh, B) Initial Cartesian Mesh, C) Final Surface Mesh

The minimum elongation of 2 in. (50.8 mm) should be calculated by the following equation: U.S. Customary Unit Equation [7]. The model's intake has automatically applied the pressure boundary condition, which is expressed mathematically as:

$$\forall \vec{v} = -v_0 \hat{n} \quad c = c_0 \qquad 8$$

where v_0 and c_0 are given the proper values in the simulations. Conditions like zero flux and no-slip are applied at the microchannel walls. These boundary conditions are expressed as follows:

$$\vec{N} = (c\vec{v} - D_{\mathrm{AB}} \nabla c). \qquad 9$$

The boundary conditions at the outlet for the flow transfer and transit equations are pressures outlet and convection flux, respectively. These equations are pertinent:

$$p = p_0 = 0; \mu\{\nabla \vec{v} + (\nabla \vec{v})^T\} \cdot \hat{n} = 0 \quad -\hat{n} \cdot D_{\mathrm{AB}} \nabla c = 0 \qquad 10$$

III. RESULTS

To address the caus"s of unidentified natural frequencies and unidentified vibration caused in the acquired findings, the piping system's finite element an'lysis is constructed using ANSYS software. The deviation laws of various order modal studies are also acquired, and the gas column frequencies of the pipeline are computed and evaluated with the vibration response. The predicted simulation vibration modes of pipes A and B are shown in Figure 3. According to the figures, pipe B vibrates both vertically and horizontally, but pipe A seems to vibrate more transversely.

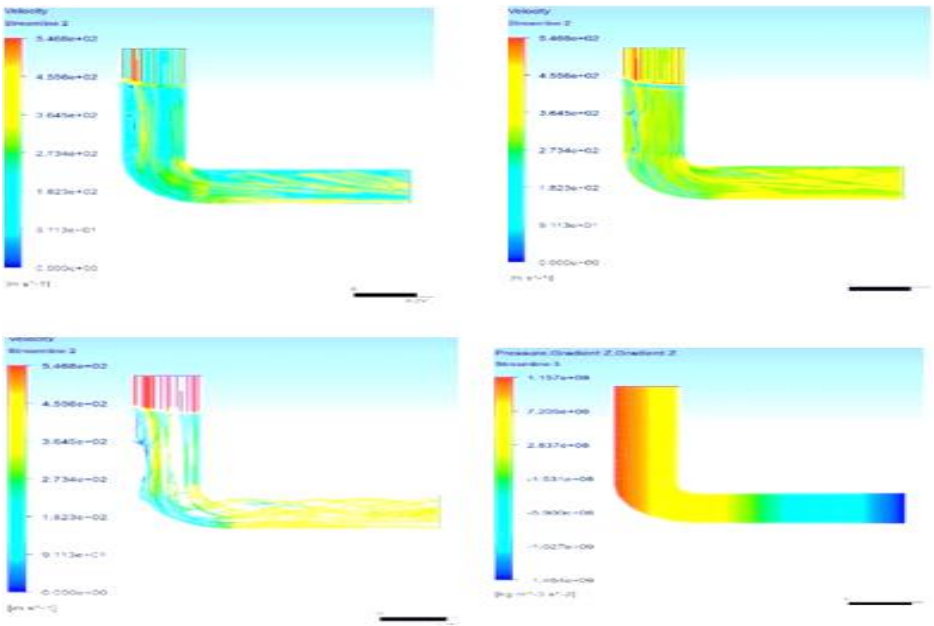

Fig 3 (A) Velocity Profile of Normal Static Enthalpy, (B) Velocity Profile of Initial Stage with a Plaque at Descending Side of the Pipe, (C) Velocity Profile of Pipe with Bypass, (D) Pressure Distribution in the Pipe, F--Pressure Distribution with High"

ISSN No:-2456-2165

Figure 3 de”icts t“e gas column contour graphs produced by simulation computing. The majority of the gas column may be seen on pipe B in picture 3. It results from pipe B's acoustic shutdown’ Through modeling, a frequency of 117.8 Hz, which is close to the vibration frequency of 116.75 Hz, is projected for it. The majority of the gas column in Figure 3(b) is on pipe A, which will have an impact on pipe B. The gas column frequency is predicted by the simulation to be 128.0 Hz, which is quite close to the field measurement of 123.0 Hz.

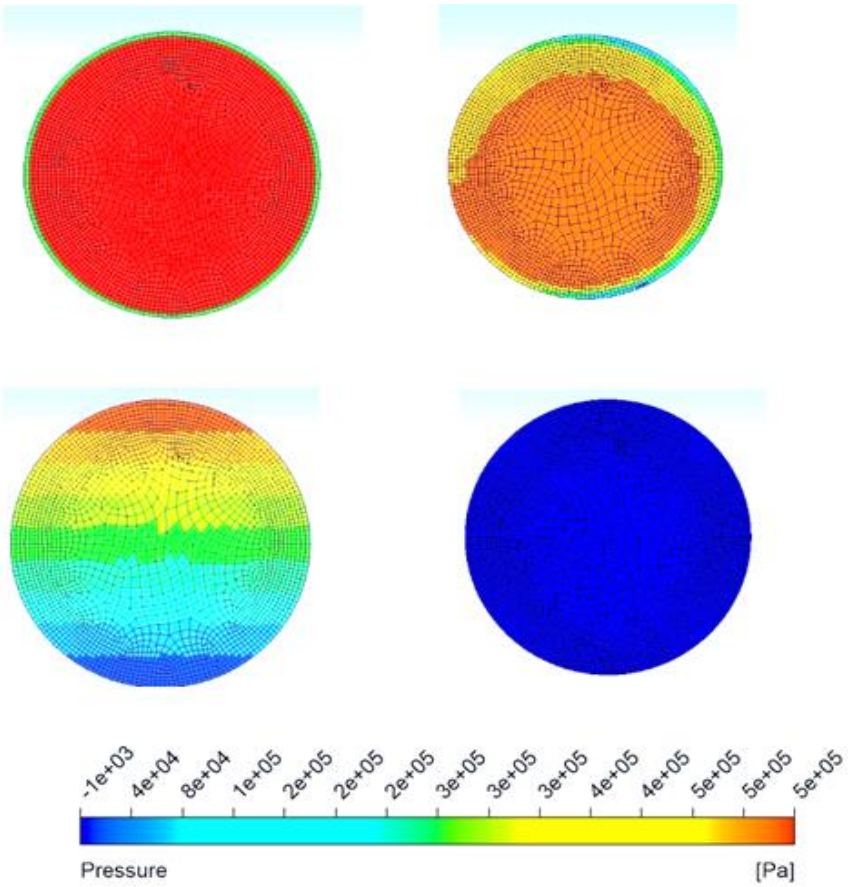

Fig 4 (A) Critical velocity of the pinned-pinned pipe as a function of the mass ratio for different lengths, (B) Effect of foundation stiffness on the natural frequency of the pinned-pinned pipe at different fluid pressures, (C) Dimensionless frequency for the lowest modes of a pipe conveying fluid, (D) Proper modes on fluid velocity function of pinned-pinned pipe conveying fluid, E-Exploration of the pipe due to high vibration.

➢ *Comparis”N Between “Ormal and Vibration Conditions:*

Figure 5 (a, b, and“c) show the time domain waveforms and spectra of MP4 under normal and vibration conditions. It can be seen from the figures that under normal conditions, the vibration is very small, while under vibration conditions, the vibration increases sharply, and the vibration frequencies are 116.75 Hz and 123.0 Hz.

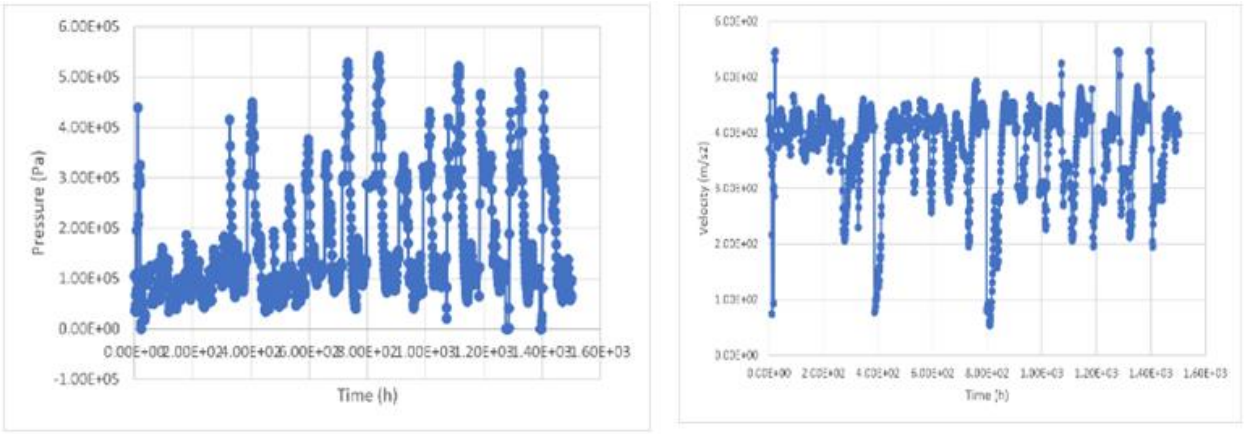

Fig 5 (A) Convergence Behavior of Residuals, (B) Convergence Behavior of Drag Coefficient, (C) Vibration Modes of Pipe

ISSN No:-2456-2165

The area-averaged void fraction fluctuation seems to be a key parameter in flow-induced vibration study. For the time domain and frequency spectrum signals of slug flow, the CFD study in this analysis is compared with the void fraction and the corresponding results obtained by previous experiments. The computational fluid dynamics prediction well represents the void fraction fluctuation of fluid flow. For the time domain and frequency spectrum signals of fluid flow, the CFD study in this analysis is compared with the void fraction and the corresponding results obtained by previous experiments.

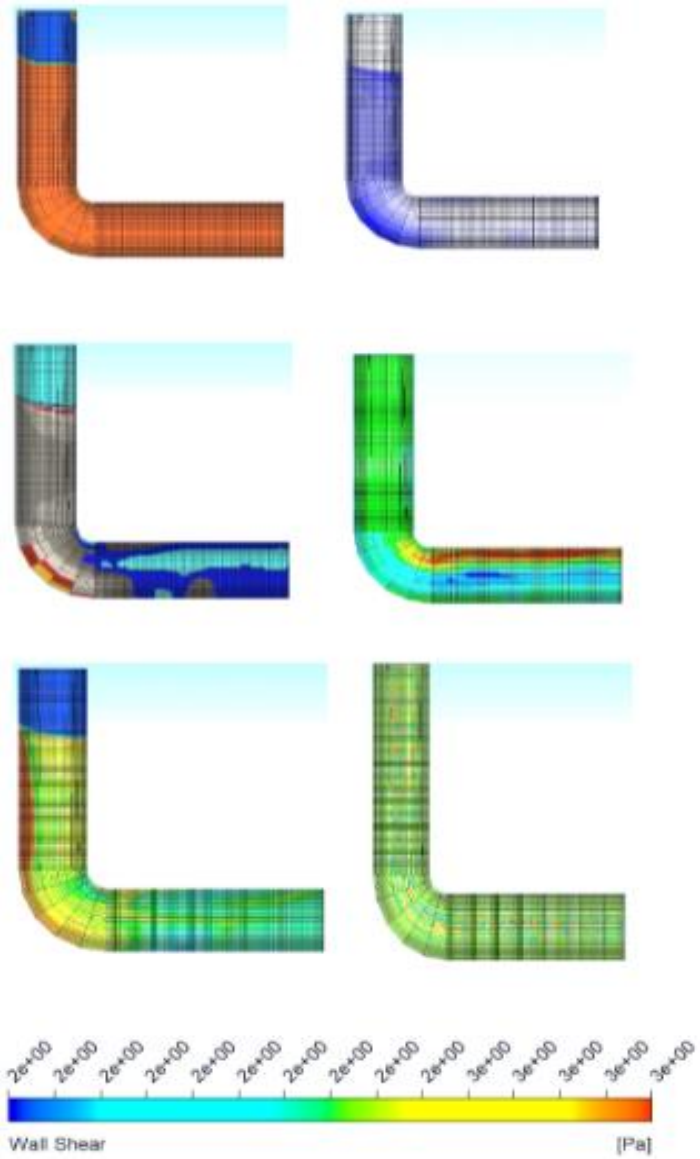

Fig 6 Shows Elastic Foundation Effect on the Variation of the First Modes as a Function of the Fluid Velocity

Table 2 The Results were Obtained by Solving the Governing Equation Through Simulation by Considering Four Elements

S no.	P=P atm, V=10m/sec, T=373k frequency (Hz)	T=423k	T=473K	T=523K
1	69.978	67.881	65.708	63.451
2	69.985	67.887	65.714	63.457
3	189.33	186.55	183.72	180.85
4	189.34	186.56	183.74	180.86

Table 3 Represents the Trend of Increasing Temperature on Frequency.

S no.	Pressure=1Mpa, velocity=10m/sec, temp=373k Simulation, Frequency (Hz)	Analytical solution Frequency (Hz)
1	69.985	72.762
2	69.991	75.313
3	189.34	165.091
4	189.35	218.472

IV. CONCLUSION

When compared to the normal pipe model in the research, the velocity was determined to be 7.5% lower in the pipe with plaque model. However, the increases in pressure and WSS were 94.9% and 74.41%, respectively. Because of this, the measured fluid pressure and WSS in the plaque model were greater than they were in the typical model. I conducted parametric studies on the effect of temperature, pressure drop, and velocity change on the frequencies. By using ANSYS for simulation purposes we can conclude that as the temperature increases by keeping other values constant, the natural frequency for the particular mode shape decreases. They kept the same value constant and increased the pressure. I examined the problem of the conveyance of hot fluid through a pipe laid in shallow waters through the study of the geometric, operational, and environmental parameters on the transverse natural frequencies of the pipeline.

We employ the transverse governing differential equation of motion in treating this problem. In the solution of the equation by using the analytical approach, we get the eigenvalues in which the imaginary part represents the frequency. Further studies may be required to identify the spectrum of instabilities so that it may bring down the excessive pressure to a normal value and the losses to a stable condition. The measurement of field vibration and the simulation computation suggest that there is a gas column excitation source in the pipeline. The gas column spreads outward along the pipeline, causing severe vibration when it comes into contact with the unreasonable pipeline. The primary vibration frequencies are 116.75 Hz as well as 123.0 Hz. The former is created by the resonance of the gas column frequency and the natural frequency in pipe B, while the latter is caused by the force of the gas column in pipe A acting on pipe B. Future studies on various pipe elbow sizes and connection angles to bending pipes are required to restore excessive vibration to standard operation.

ACKNOWLEDGMENT

To minimize pipeline vibration, it is advised that the stiffness of the underground pipe portion in pipe B be increased and the length of the straight pipe section between the tee and the elbow in pipe A be changed.

REFERENCES

[1]. Z.I. Al-Hashimy, H.H. Al-Kayiem, R.W. Time, Experimental investigation on the vibration induced by slug flow in horizontal pipe, ARPN J. Eng. Appl. Sci. 11 (2016).

[2]. M. Kheiri, M.P. Païdoussis, Dynamics and stability of a flexible pinned-free cylinder in axial flow, J. Fluids Struct. 55 (2015). https://doi.org/10.1016/j.jfluidstructs.2015.02.013.

[3]. B.N. Murthy, R.B. Kasundra, J.B. Joshi, Hollow self-inducing impellers for gas-liquid-solid dispersion: Experimental and computational study, Chem. Eng. J. 141 (2008). https://doi.org/10.1016/j.cej.2008.01.040.

[4]. Q. Deng, D. Zhu, Z. Han, L. Wang, Stress and deformation analysis of pipeline when piping routing is parallel to sliding direction of landslide, Electron. J. Geotech. Eng. 19 (2014).

[5]. W.C. Haneberg, C.A. Devine, D.N. Vázquez Feregrino, M. Orozco Calderón, Optimization of deep-water pipeline routes in areas of geologic complexity - An example from the Southern Gulf of Mexico, in: Front. Offshore Geotech. III - 3rd Int. Symp. Front. Offshore Geotech. ISFOG 2015, 2015. https://doi.org/10.1201/b18442-139.

[6]. B. Mediano-Valiente, M.I. García-Planas, Stability analysis of a clamped-pinned pipeline conveying fluid, WSEAS Trans. Syst. 13 (2014).

[7]. R.A. Ibrahim, Overview of mechanics of pipes conveying fluids-part I: Fundamental studies, J. Press. Vessel Technol. Trans. ASME. 132 (2010). https://doi.org/10.1115/1.4001271.

[8]. O. Doaré, E. De Langre, Effect of length on the instability of hanging pipes, in: ASME Int. Mech. Eng. Congr. Expo. Proc., 2002. https://doi.org/10.1115/IMECE2002-39018.

[9]. O. Doaré, E. de Langre, The role of boundary conditions in the instability of one-dimensional systems, Eur. J. Mech. B/Fluids. 25 (2006). https://doi.org/10.1016/j.euromechflu.2006.01.001.

[10]. C.W. Bert, T.L.C. Chen, Wave propagation in fluid-conveying piping constructed of composite material, J. Press. Vessel Technol. Trans. ASME. 97 (1975). https://doi.org/10.1115/1.3454292.

[11]. Effects of Attached Mass on Stability of Pipe Conveying Fluid with Crack, Trans. Korean Soc. Noise Vib. Eng. 17 (2007). https://doi.org/10.5050/ksnvn.2007.17.10.1002.

[12]. K.R. Chellapilla, H.S. Simha, Critical velocity of fluid-conveying pipes resting on two-parameter foundation, J. Sound Vib. 302 (2007). https://doi.org/10.1016/j.jsv.2006.11.007.

[13]. P. Chuang, D.L. Smith, Elastic Analysis of Submarine Pipelines, J. Struct. Eng. 118 (1992). https://doi.org/10.1061/(asce)0733-9445(1992)118:1(90).

[14]. R.A.M. Silveira, C.L. Nogueira, P.B. Gonçalves, A numerical approach for equilibrium and stability analysis of slender arches and rings under contact constraints, Int. J. Solids Struct. 50 (2013). https://doi.org/10.1016/j.ijsolstr.2012.09.015.

[15]. P. Gao, B.W. Jin, J. Zeng, Y.T. Zhan, H. Zhou, Numerical analysis of deep-water pipeline abandonment and recovery, J. Mar. Sci. Technol. 27 (2019). https://doi.org/10.6119/JMST.201912_27(6).0003.